mathematics

MDPI

Article

Dynamical Visualization and Qualitative Analysis of the (4+1)-Dimensional KdV-CBS Equation Using Lie Symmetry Analysis

Maria Luz Gandarias [1], Nauman Raza [2,*], Muhammad Umair [3] and Yahya Almalki [4]

[1] Department of Mathematics, University of Cadiz, 11510 Puerto Real, Spain; marialuz.gandarias@uca.es
[2] Department of Mathematics, University of the Punjab, Quaid-e-Azam Campus, Lahore 54590, Pakistan
[3] Department of Mathematics, University of Engineering and Technology, Lahore 54890, Pakistan; mrumair11234@gmail.com
[4] Department of Mathematics, College of Science, King Khalid University, Abha 61413, Saudi Arabia; yalmalki@kku.edu.sa
* Correspondence: nauman.math@pu.edu.pk

Abstract: This study investigates novel optical solitons within the intriguing (4+1)-dimensional Korteweg–de Vries–Calogero–Bogoyavlenskii–Schiff (KdV-CBS) equation, which integrates features from both the Korteweg–de Vries and the Calogero–Bogoyavlenskii–Schiff equations. Firstly, all possible symmetry generators are found by applying Lie symmetry analysis. By using these generators, the given model is converted into an ordinary differential equation. An adaptive approach, the generalized exp(-$\mathfrak{G}(\chi)$) expansion technique has been utilized to uncover closed-form solitary wave solutions. The findings reveal a range of soliton types, including exponential, rational, hyperbolic, and trigonometric functions, represented as bright, singular, rational, periodic, and new solitary waves. These results are illustrated numerically and accompanied by insightful physical interpretations, enriching the comprehension of the complex dynamics modeled by these equations. Our approach's novelty lies in applying a new methodology to this problem, yielding a variety of novel optical soliton solutions. Additionally, we employ bifurcation and chaos techniques for a qualitative analysis of the model, extracting a planar system from the original equation and mapping all possible phase portraits. A thorough sensitivity analysis of the governing equation is also presented. These results highlight the effectiveness of our methodology in tackling nonlinear problems in both mathematics and engineering, surpassing previous research efforts.

Keywords: (4+1)-D KdV–CBS equation; generalized exp(-$\mathfrak{G}(\chi)$) expansion method; novel solitons; dynamic study of bifurcation and chaotic behavior; sensitivity analysis

MSC: 35C08; 34F10

Academic Editor: Carlo Bianca

Received: 11 November 2024
Revised: 16 December 2024
Accepted: 23 December 2024
Published: 29 December 2024

Citation: Gandarias, M.L.; Raza, N.; Umair, M.; Almalki, Y. Dynamical Visualization and Qualitative Analysis of the (4+1)-Dimensional KdV-CBS Equation Using Lie Symmetry Analysis. *Mathematics* **2025**, *13*, 89. https://doi.org/10.3390/math13010089

1. Introduction

Nonlinear phenomena manifest across various domains such as physics, engineering, chemistry, biological sciences, and computational mathematics. Nonlinear partial differential equations (NLPDEs) perform a vital role in modeling and simulating these circumstances [1,2]. Over the last three decades, significant research has been devoted to nonlinear evolution equations (NLEEs), which are highly relevant in numerous scientific disciplines, including quantum mechanics, condensed matter physics, plasma physics, fluid mechanics, and nonlinear optical fiber [3,4]. The formation of solitons is commonly a

result of the interplay between nonlinear effects and dispersion. Notable advancements have occurred in the field since the first application of soliton theory to NLPDEs. Analysts have made significant strides in finding traveling wave patterns by analyzing a variety of components. Wave patterns that maintain their shape while propagating are known as solitary waves. Such phenomena appear in different disciplines like optics, fluid mechanics, biology, and atomic physics [5,6]. Several successful approaches have been developed to find soliton solutions for NLPDEs: the unified method, the singular manifold approach, the exponential expansion scheme, and much more [7–9].

In 1895, Diederik Korteweg and Gustav de Vries conducted an in-depth study of the Korteweg–de Vries (KdV) equation [10], which theoretically demonstrated the existence of solitons. Wave propagation in water is described by the integrable system known as the KdV equation. Due to the entire integrability of the single-dimensional KdV equation and its utmost applicability in optical science or plasma dynamics, a wealth of work has been devoted to different results on KdV-type equations [11,12]. The Calogero–Bogoyavlenskii–Schiff (CBS) equation is a type of nonlinear evolution equation first developed by Bogoyavlenskii [13] and Schiff [14]. Later, researchers derived the CBS equation by differentiating the KdV equation [15]. This equation can describe various nonlinear processes in fluid mechanics and plasma physics, which received plenty of interest [16,17].

In higher dimensions, the CBS equation serves an essential part in examining the interactions of long waves within media exhibiting nonlinear dispersion [18]. The (4+1)-D Korteweg–de Vries–Calogero–Bogoyavlenskii–Schiff (KdV-CBS) equation investigated in this work combines features of both the KdV and CBS equations and is integrated via the bilinear method [19]. This equation advances our comprehension of high-dimensional integrable systems, offering valuable insights into the dynamics and interaction of nonlinear wave phenomena in plasma physics and fluid mechanics [20]. The (4+1)-D KdV-CBS equation is formulated as follows:

$$\begin{aligned} &4\mathcal{E}_{xt} + \epsilon(6\mathcal{E}_x\mathcal{E}_{xx} + \mathcal{E}_{xxxx}) + \alpha(4\mathcal{E}_x\mathcal{E}_{xy} + 2\mathcal{E}_{xx}\mathcal{E}_y + \mathcal{E}_{xxxy}) + \\ &\beta(4\mathcal{E}_x\mathcal{E}_{xz} + 2\mathcal{E}_{xx}\mathcal{E}_z + \mathcal{E}_{xxxz}) + \gamma(4\mathcal{E}_x\mathcal{E}_{xs} + 2\mathcal{E}_{xx}\mathcal{E}_s + \mathcal{E}_{xxxs}) + \\ &a\mathcal{E}_{xx} + b\mathcal{E}_{xy} + c\mathcal{E}_{xz} + d\mathcal{E}_{xs} = 0. \end{aligned} \tag{1}$$

The function $\mathcal{E} = \mathcal{E}(t, x, y, z, s)$ represents an unknown variable. Eight arbitrary variables are represented by the following values: a, b, c, d, α, β, γ, and ϵ. Equation (1) can be reduced to other nonlinear integrable equations, each with uniquely significant physical properties. Specifically, setting $\alpha = \beta = \gamma = 0$ transforms Equation (1) into a (4+1)-D KdV equation. Similarly, by taking $a = b = c = d = \epsilon = 0$, Equation (1) simplifies into a (4+1)-D CBS equation. One of the most reliable strategies for constructing solutions to NLPDEs is the application of Lie group transformation theory. Symmetry methods applied to NLPDEs facilitate reductions and the discovery of invariant solutions. Specifically, invariant solutions are often useful for analyzing the analytical properties of PDEs. It is well understood that conservation laws are essential to the solution of NLPDEs. While not every conservation law for a PDE may have a direct physical meaning, they are crucial for examining the integrability of the equations.

In this study, we focus on Equation (1) through the lens of symmetry reduction theory in PDEs. We acquire low-order conservation laws for Equation (1) and derive the Lie point symmetries accepted by it for arbitrary constants. By leveraging the relationship between conservation laws and symmetries and applying the multiplier method to a reduced ODE, we directly derive a fourth-order ODE. Using the two derived conservation laws, we acquire the two first integrals. Incorporating these integrals enables us to achieve a triple reduction, simplifying the problem to a second-order autonomous equation. The generalized exp(-$\mathfrak{S}(\chi)$) expansion method (GEM) is a powerful tool used to deal with

NLPDEs, providing a wide array of novel solitary wave solutions. Our goal is to widen its application to investigate NLEEs, with a particular focus on the (4+1)-D KdV-CBS equation. We aim to uncover a range of solution types, such as rational, hyperbolic, exponential, and trigonometric forms. The novelty of this approach exists in its previously unverified application to these equations, which is expected to improve the method's elegance and reliability, as demonstrated in earlier studies [21,22]. We anticipate that our research will advance knowledge of the dynamics of waves in dispersive media.

Moreover, we employed bifurcation analysis to further our understanding of the planar dynamical system derived from the arguing system [23,24]. Bifurcation analysis, a field that has gained high interest in the latest research, explores how dynamical systems depend on underlying physical characteristics. Finally, we conducted a sensitivity analysis of the mathematical model to examine its responsiveness to parameter variations [25,26]. Our research delves deeply into nonlinear periodic traveling waves, a topic that has been largely unexamined in previous work, thereby contributing significant insights to the field. This paper is organized as follows: Section 2 focuses on the mathematical analysis of the arguing system to derive the ODE. Section 3 details the generalized exp(-$\mathfrak{G}(\chi)$) expansion method. Section 4 presents the results along with graphical representations. In Sections 5 and 6, a qualitative evaluation of the model is carried out. Section 7 discusses sensitivity analysis, and the conclusion, including future research suggestions, is provided in Section 8.

2. Traveling Wave Reduction and First Integrals from Symmetry Reduction

The reduction to a traveling wave ODE is arguably among the most popular uses of symmetry reduction. The form of a traveling wave is:

$$\mathcal{E}(t,x,y,z,s) = \mathcal{V}(\chi) \quad \chi = x + b_1 y + b_2 z + b_3 s - b_4 t, \tag{2}$$

where b_1, b_2, b_3, and b_4 are constants. Inserting the traveling wave pattern (2) in Equation (1) results in a nonlinear fourth-order ODE.

$$(\alpha b_1 + \beta b_2 + \gamma b_3 + \epsilon)\mathcal{V}'''' + \big(6(\alpha b_1 + \beta b_2 + \gamma b_3 + \epsilon)\mathcal{V}' + (bb_1 + cb_2 + db_3 + a - 4b_4)\big)\mathcal{V}'' = 0. \tag{3}$$

Since this ODE arises from a symmetry reduction under translations of Equation (1), the corresponding conservation laws of the equation invariant under translations will similarly reduce. Furthermore, all first integrals arising from symmetry-invariant conservation laws can be found directly using the symmetry through the general multi-reduction method introduced in [27,28].

Setting $\mathcal{V}' = \mathcal{F}$ yields the nonlinear third-order ODE.

$$(\alpha b_1 + \beta b_2 + \gamma b_3 + \epsilon)\mathcal{F}''' + (6(\alpha b_1 + \beta b_2 + \gamma b_3 + \epsilon)\mathcal{F} + (bb_1 + cb_2 + db_3 + a - 4b_4))\mathcal{F}' = 0. \tag{4}$$

Upon searching for all the multipliers of Equation (4), only the following three multipliers arise:

$$M_1 = 1, \quad M_2 = \mathcal{F}, \quad M_3 = \mathcal{F}'' + 3\mathcal{F}^2.$$

These multipliers correspond to invariants under translation multipliers of Equation (4), and the corresponding first integrals are given by the following:

$$\begin{aligned}
\mathcal{T}_1 &= (\alpha b_1 + \beta b_2 + \gamma b_3 + \epsilon)\mathcal{F}'' + 3(\alpha b_1 + \beta b_2 + \gamma b_3 + \epsilon)\mathcal{F}^2) + C = C_1, \\
\mathcal{T}_2 &= (\alpha b_1 + \beta b_2 + \gamma b_3 + \epsilon)\left(\mathcal{F}\mathcal{F}'' - \frac{1}{2}(\mathcal{F}')^2 + 2\mathcal{F}^3\right) + \frac{1}{2}(bb_1 + cb_2 + db_3 + a - 4b_4)\mathcal{F}^2 = C_2,
\end{aligned} \tag{5}$$

$$\begin{aligned}\mathcal{T}_3 &= (\alpha b_1 + \beta b_2 + \gamma b_3 + \epsilon)\left(\tfrac{1}{2}(\mathcal{F}'')^2 + 3\mathcal{F}^2\mathcal{F}'' + \tfrac{9}{2}\mathcal{F}^4\right)\\ &+(bb_1 + cb_2 + db_3 + a - 4b_4)\left(\tfrac{1}{2}(\mathcal{F}')^2 + \mathcal{F}^3\right) = C_3.\end{aligned} \tag{6}$$

The two functionally independent first integrals arise from M_1 and M_2. Eliminating $\mathcal{F}''$ yields a first-order ODE.

$$\mathcal{F}'^2 + 2\mathcal{F}^3 - \frac{bb_1 + cb_2 + db_3 + a - 4b_4}{\alpha b_1 + \beta b_2 + \gamma b_3 + \epsilon}\mathcal{F}^2 + \frac{2C_3 - 2C_2\mathcal{F}}{\alpha b_1 + \beta b_2 + \gamma b_3 + \epsilon} = 0. \tag{7}$$

Consequently, we achieved a reduction in one step from the third-order PDE to a first-order ODE. Equation (7) can be obtained, and integrating once with respect to χ yields the solution of (4).

3. Analysis of the Governing Method

Here, we provide a summary of the GEM, which we use to find new solitary wave solutions for the NLSE [21,22]. We start by examining a general NLPDE, expressed as follows:

$$\mathcal{O}(\mathcal{E}, \mathcal{E}_t, \mathcal{E}_x, \mathcal{E}_{tx}, \mathcal{E}_{xx}, \ldots) = 0, \tag{8}$$

where polynomial $\mathcal{O}$ contains $\mathcal{E}(x,t)$ along with its derivatives $\mathcal{E}_t, \mathcal{E}_x, \mathcal{E}_{tx}, \mathcal{E}_{xx}$, and continued. Consider the traveling wave transformation that reduces PDE to the following ODE:

$$\mathcal{G}\left(\mathcal{V}, \mathcal{V}', \mathcal{V}'', \mathcal{V}''', \ldots\right) = 0. \tag{9}$$

The GEM core steps are summarized as follows:

Step 1: By using the traveling wave transformation, the given PDE (8) can be changed into the ODE (9).
Step 2: The $\aleph$ is determined using the balance principle, which ensures equilibrium between the highest-order derivative and the dominant nonlinear component in Equation (7).
Step 3: Assume that the suggested trial solution for the given ODE can be written as follows:

$$\mathcal{P}(\chi) = \sum_{j=0}^{\aleph} a_j \left[\exp\left(-\frac{\mathcal{P}_1\mathfrak{S}(\chi) + \mathcal{P}_2}{\mathcal{P}_3\mathfrak{S}(\chi) + \mathcal{P}_4}\right)\right]^j. \tag{10}$$

Here, the constants $a_j (j = 0, 1, \ldots \aleph)$ are to be determined, subject to the condition that $a_j \neq 0$, and $\mathfrak{S}$ must satisfy the differential equation:

$$\mathfrak{S}'(\chi) = \frac{(\mathcal{P}_3\mathfrak{S}(\chi) + \mathcal{P}_4)^2}{(\mathcal{P}_1\mathcal{P}_4 - \mathcal{P}_2\mathcal{P}_3)}\left(\exp\left(-\frac{\mathcal{P}_1\mathfrak{S}(\chi) + \mathcal{P}_2}{\mathcal{P}_3\mathfrak{S}(\chi) + \mathcal{P}_4}\right) + \mathcal{Q}_1 \exp\left(\frac{\mathcal{P}_1\mathfrak{S}(\chi) + \mathcal{P}_2}{\mathcal{P}_3\mathfrak{S}(\chi) + \mathcal{P}_4}\right) + \mathcal{Q}_2\right). \tag{11}$$

When $\mathcal{P}_1\mathcal{P}_4 - \mathcal{P}_2\mathcal{P}_3 \neq 0$, the families of solutions for Equation (9) are as follows:

Family 1: When $(\mathcal{P}_1\mathcal{P}_4 - \mathcal{P}_2\mathcal{P}_3) \neq 0$, $\mathcal{Q}_1 \neq 0$, $\Delta = (\mathcal{Q}_2^2 - 4\mathcal{Q}_1) > 0$, $\mathcal{P}_2 = 0$,

$$\mathfrak{S}_1(\varsigma) = \frac{\mathcal{P}_4 \ln\left(\frac{-\sqrt{\mathcal{Q}_2^2 - 4\mathcal{Q}_1}\tanh\left(\frac{1}{2}\sqrt{\mathcal{Q}_2^2 - 4\mathcal{Q}_1}(C+\chi)\right) - \mathcal{Q}_2}{2\mathcal{Q}_1}\right)}{\mathcal{P}_1 - \mathcal{P}_3 \ln\left(\frac{-\sqrt{\mathcal{Q}_2^2 - 4\mathcal{Q}_1}\tanh\left(\frac{1}{2}\sqrt{\mathcal{Q}_2^2 - 4\mathcal{Q}_1}(C+\chi)\right) - \mathcal{Q}_2}{2\mathcal{Q}_1}\right)}. \tag{12}$$

Family 2: When $(\mathcal{P}_1\mathcal{P}_4 - \mathcal{P}_2\mathcal{P}_3) \neq 0$, $\mathcal{Q}_1 \neq 0$, $\Delta = (\mathcal{Q}_2^2 - 4\mathcal{Q}_1) < 0$, $\mathcal{P}_2 = 0$,

$$\mathfrak{S}_2(\varsigma) = \frac{\mathcal{P}_4 \ln\left(\frac{\sqrt{4\mathcal{Q}_1 - \mathcal{Q}_2^2}\tan\left(\frac{1}{2}\sqrt{4\mathcal{Q}_1 - \mathcal{Q}_2^2}(C+\chi)\right) - \mathcal{Q}_2}{2\mathcal{Q}_1}\right)}{\mathcal{P}_1 - \mathcal{P}_3 \ln\left(\frac{\sqrt{4\mathcal{Q}_1 - \mathcal{Q}_2^2}\tan\left(\frac{1}{2}\sqrt{4\mathcal{Q}_1 - \mathcal{Q}_2^2}(C+\chi)\right) - \mathcal{Q}_2}{2\mathcal{Q}_1}\right)}. \tag{13}$$

Family 3: When $(\mathcal{P}_1\mathcal{P}_4 - \mathcal{P}_2\mathcal{P}_3) \neq 0$, $\mathcal{Q}_1 \neq 0$, $\mathcal{Q}_2 \neq 0$, $\Delta = (\mathcal{Q}_2^2 - 4\mathcal{Q}_1) = 0$, $\mathcal{P}_2 = 0$,

$$\mathfrak{S}_3(\varsigma) = \frac{\mathcal{P}_4 \ln\left(-\frac{2\mathcal{Q}_2(C+\chi)+2}{\mathcal{Q}_2^2(C-\Omega t+x)}\right)}{\mathcal{P}_1 - \mathcal{P}_3 \ln\left(-\frac{2\mathcal{Q}_2(C+\chi)+2}{\mathcal{Q}_2^2(C-\Omega t+x)}\right)}. \tag{14}$$

Family 4: When $(\mathcal{P}_1\mathcal{P}_4 - \mathcal{P}_2\mathcal{P}_3) \neq 0$, $\mathcal{Q}_1 \neq 0$, $\mathcal{Q}_2 \neq 0$, $\Delta = (\mathcal{Q}_2^2 - 4\mathcal{Q}_1) > 0, \mathcal{P}_3 = 0$,

$$\mathfrak{S}_4(\varsigma) = \frac{\mathcal{P}_4 \ln\left(\frac{-\sqrt{e^{\frac{2\mathcal{P}_2}{\mathcal{P}_4}}\left(\mathcal{Q}_2{}^2 - 4\mathcal{Q}_1\right)}\tanh\left(\frac{1}{2}\sqrt{\mathcal{Q}_2{}^2 - 4\mathcal{Q}_1}(C+\chi)\right) - \mathcal{Q}_2 e^{\frac{\mathcal{P}_2}{\mathcal{P}_4}}}{2\mathcal{Q}_1}\right)}{\mathcal{P}_1} - \frac{2\mathcal{P}_2}{\mathcal{P}_1}. \tag{15}$$

Family 5: When $(\mathcal{P}_1\mathcal{P}_4 - \mathcal{P}_2\mathcal{P}_3) \neq 0$, $\mathcal{Q}_1 \neq 0$, $\mathcal{Q}_2 \neq 0$, $\Delta = (\mathcal{Q}_2^2 - 4\mathcal{Q}_1) < 0, \mathcal{P}_3 = 0$,

$$\mathfrak{S}_5(\varsigma) = \frac{\mathcal{P}_4 \ln\left(\frac{-\sqrt{e^{\frac{2\mathcal{P}_2}{\mathcal{P}_4}}\left(4\mathcal{Q}_1 - \mathcal{Q}_2{}^2\right)}\tan\left(\frac{1}{2}\sqrt{4\mathcal{Q}_1 - \mathcal{Q}_2{}^2}(C+\chi)\right) - \mathcal{Q}_2 e^{\frac{\mathcal{P}_2}{\mathcal{P}_4}}}{2\mathcal{Q}_1}\right)}{\mathcal{P}_1} - \frac{2\mathcal{P}_2}{\mathcal{P}_1}. \tag{16}$$

Family 6: When $(\mathcal{P}_1\mathcal{P}_4 - \mathcal{P}_2\mathcal{P}_3) \neq 0$, $\mathcal{Q}_1 \neq 0$, $\mathcal{Q}_2 \neq 0$, $\Delta = (\mathcal{Q}_2^2 - 4\mathcal{Q}_1) = 0, \mathcal{P}_3 = 0$,

$$\mathfrak{S}_6(\varsigma) = \frac{\mathcal{P}_4 \ln\left(\frac{2\mathcal{Q}_2(C+\chi)+2}{\mathcal{Q}_2^2(C+\chi)}\right)}{\mathcal{P}_1} - \frac{\mathcal{P}_2}{\mathcal{P}_1}. \tag{17}$$

Family 7: When $(\mathcal{P}_1\mathcal{P}_4 - \mathcal{P}_2\mathcal{P}_3) \neq 0$, $\mathcal{Q}_1 = 0$, $\mathcal{Q}_2 \neq 0$, $\Delta = (\mathcal{Q}_2^2 - 4\mathcal{Q}_1) > 0$,

$$\mathfrak{S}_7(\varsigma) = -\frac{\mathcal{P}_4 \ln\left(\frac{\mathcal{Q}_2}{e^{\mathcal{Q}_2(C+\chi)} - 1}\right) + \mathcal{P}_2}{\mathcal{P}_3 \ln\left(\frac{\mathcal{Q}_2}{e^{\mathcal{Q}_2(C+\chi)} - 1}\right) + \mathcal{P}_1}. \tag{18}$$

Family 8: When $(\mathcal{P}_1\mathcal{P}_4 - \mathcal{P}_2\mathcal{P}_3) \neq 0$, $\mathcal{Q}_2 = 0, \mathcal{Q}_1 = 0$, $\Delta = (\mathcal{Q}_2^2 - 4\mathcal{Q}_1) = 0$,

$$\mathfrak{S}_8(\varsigma) = -\frac{\mathcal{P}_2 - \mathcal{P}_4 \ln(C+\chi)}{\mathcal{P}_1 - \mathcal{P}_3 \ln(C+\chi)}. \tag{19}$$

Family 9: When $(\mathcal{P}_1\mathcal{P}_4 - \mathcal{P}_2\mathcal{P}_3) \neq 0$, $\mathcal{Q}_1 \neq 0$, $\mathcal{Q}_2 \neq 0$, $\Delta = (\mathcal{Q}_2^2 - 4\mathcal{Q}_1) = 0$, $\mathcal{P}_f \neq 0$ $(f = 1, 2, 3, 4)$,

$$\mathfrak{S}_9(\varsigma) = -\frac{\mathcal{P}_2 - \mathcal{P}_4 \ln\left(-\frac{2(C+\chi)}{\mathcal{Q}_2(C+\chi)-2}\right)}{\mathcal{P}_1 - \mathcal{P}_3 \ln\left(-\frac{2(C+\chi)}{\mathcal{Q}_2(C+\chi)-2}\right)}. \tag{20}$$

Family 10: When $(\mathcal{P}_1\mathcal{P}_4 - \mathcal{P}_2\mathcal{P}_3) \neq 0$, $\mathcal{Q}_1 < 0$, $\mathcal{Q}_2 = 0$,

$$\mathfrak{S}_{10}(\varsigma) = -\frac{\mathcal{P}_2 - \mathcal{P}_4 \ln\left(-\frac{e^{-2\sqrt{-\mathcal{Q}_1}(C+\chi)}+1}{\sqrt{-\mathcal{Q}_1}e^{-2\sqrt{-\mathcal{Q}_1}(C+\chi)}-1}\right)}{\mathcal{P}_1 - \mathcal{P}_3 \ln\left(-\frac{e^{-2\sqrt{-\mathcal{Q}_1}(C+\chi)}+1}{\sqrt{-\mathcal{Q}_1}e^{-2\sqrt{-\mathcal{Q}_1}(C+\chi)}-1}\right)}. \tag{21}$$

Step 4: Swapping Equation (10) in the offered ODE, applying Equation (11), and then setting the coefficients of $\left(\exp\left(-\frac{\mathcal{P}_1\mathfrak{S}(\chi)+\mathcal{P}_2}{\mathcal{P}_3\mathfrak{S}(\chi)+\mathcal{P}_4}\right)\right)^j$ in the resulting system to zero, an algebraic equation set for $\mathcal{P}_1, \mathcal{P}_2, \mathcal{P}_3, \mathcal{P}_4$, $\mathcal{Q}_1$, $\mathcal{Q}_2$, and $a_j (j = 0, 1, \ldots \aleph)$ is generated.
Step 5: Considering the values of the constants $\mathcal{P}_1, \mathcal{P}_2, \mathcal{P}_3, \mathcal{P}_4$, $\mathcal{Q}_1$, $\mathcal{Q}_2$, and a_j can be determined by dealing with the algebraic equations by proceeding from step 4. Since the solutions for Equation (11) are already well-known, we substitute the obtained values of $\mathcal{P}_1, \mathcal{P}_2, \mathcal{P}_3, \mathcal{P}_4$, $\mathcal{Q}_1$, $\mathcal{Q}_2$, and a_j, along with these consequences, into Equation (10). This enables us to generate novel soliton solutions for the NLPDE in Equation (8).

Application

Here, we apply the GEM to obtain the new solitary wave patterns for the NLEE found from Equation (7). We determine that $\aleph$ is one using the HB in Equation (7). As a result, the trial solution of Equation (10) becomes as follows:

$$\mathcal{P}(\chi) = a_0 + a_1 \exp\left(-\frac{\mathcal{P}_1\mathfrak{S}(\chi) + \mathcal{P}_2}{\mathcal{P}_3\mathfrak{S}(\chi) + \mathcal{P}_4}\right). \tag{22}$$

The constants $\mathcal{P}_1, \mathcal{P}_2, \mathcal{P}_3$, and $\mathcal{P}_4$ are arbitrary. By omitting Equation (22) with Equation (11) in Equation (7), we generate a polynomial of the form $\left[\exp\left(-\frac{\mathcal{P}_1\mathfrak{S}(\chi)+\mathcal{P}_2}{\mathcal{P}_3\mathfrak{S}(\chi)+\mathcal{P}_4}\right)\right]^j$ for $j = 0, 1, 2, 3, \ldots \aleph$. We then set all the polynomial coefficients to zero, leading to a system of algebraic equations for b_1, b_2, b_3, b_4, $a_0, a_1, \mathcal{P}_1, \mathcal{P}_2, \mathcal{P}_3, \mathcal{P}_4, \mathcal{Q}_1$, and $\mathcal{Q}_2$. Using Mathematica version 13, this system can be solved to ascertain the values of these variables, listed as follows:

$$\begin{array}{l} a_2 = -2, C_2 = -\frac{1}{4}(a_0 + 2\mathcal{Q}_1)\left(a_1^2 + 12a_0 + 8\mathcal{Q}_1\right)(\alpha b_1 + \beta b_2 + \gamma b_3 + \epsilon), \\ C_3 = -\frac{1}{8}\left(a_1^2 + 8a_0\right)(a_0 + 2\mathcal{Q}_1)^2(\alpha b_1 + \beta b_2 + \gamma b_3 + \epsilon), \mathcal{Q}_2 = -\frac{a_1}{2}, \\ b_4 = \frac{1}{4}(a + bb_1 + cb_2 + db_3 - 8\mathcal{Q}_1(\alpha b_1 + \beta b_2 + \gamma b_3 + \epsilon)) \\ -\frac{1}{16}\left(a_1^2 + 24a_0\right)(\alpha b_1 + \beta b_2 + \gamma b_3 + \epsilon). \end{array} \tag{23}$$

Substituting Equation (23) in Equation (22) and employing Equation (2), the following expression is obtained:

$$\mathcal{E} = a_0 + e^{-\frac{2\left(A_1\Phi(\chi)+A_2\right)}{A_3\Phi(\chi)+A_4}}\left(a_1 e^{\frac{A_1\Phi(\chi)+A_2}{A_3\Phi(\chi)+A_4}} - 2\right). \tag{24}$$

As a result, we derive the novel solitary wave solution for the NLPDE from Equation (1) utilizing Equation (12) through Equation (21). Hence, the following cases arise:

Case 1: When $(\mathcal{P}_1\mathcal{P}_4 - \mathcal{P}_2\mathcal{P}_3) \neq 0$, $\mathcal{Q}_1 \neq 0$, $\Delta = (\mathcal{Q}_2^2 - 4\mathcal{Q}_1) > 0$, $\mathcal{P}_2 = 0$,

$$\mathcal{E}_1 = a_0 - \frac{2\mathcal{Q}_1\left(a_1\left(\sqrt{\mathcal{Q}_2^2 - 4\mathcal{Q}_1}\tanh\left(\frac{1}{2}\sqrt{\mathcal{Q}_2^2 - 4\mathcal{Q}_1}(C+\chi)\right) + \mathcal{Q}_2\right) + 4\mathcal{Q}_1\right)}{\left(\sqrt{\mathcal{Q}_2^2 - 4\mathcal{Q}_1}\tanh\left(\frac{1}{2}\sqrt{\mathcal{Q}_2^2 - 4\mathcal{Q}_1}(C+\chi)\right) + \mathcal{Q}_2\right)^2}, \tag{25}$$

where $\chi = x + b_1 y + b_2 z + b_3 s - b_4 t$.

Case 2: When $(\mathcal{P}_1\mathcal{P}_4 - \mathcal{P}_2\mathcal{P}_3) \neq 0$, $\mathcal{Q}_1 \neq 0$, $\Delta = (\mathcal{Q}_2^2 - 4\mathcal{Q}_1) < 0$, $\mathcal{P}_2 = 0$,

$$\mathcal{E}_2 = a_0 - \frac{2\mathcal{Q}_1\left(a_1\left(\mathcal{Q}_2 - \sqrt{4\mathcal{Q}_1 - \mathcal{Q}_2^2}\tan\left(\frac{1}{2}\sqrt{4\mathcal{Q}_1 - \mathcal{Q}_2^2}(C+\chi)\right)\right) + 4\mathcal{Q}_1\right)}{\left(\mathcal{Q}_2 - \sqrt{4\mathcal{Q}_1 - \mathcal{Q}_2^2}\tan\left(\frac{1}{2}\sqrt{4\mathcal{Q}_1 - \mathcal{Q}_2^2}(C+\chi)\right)\right)^2}, \tag{26}$$

where $\chi = x + b_1 y + b_2 z + b_3 s - b_4 t$.
Case 3: When $(\mathcal{P}_1\mathcal{P}_4 - \mathcal{P}_2\mathcal{P}_3) \neq 0$, $\mathcal{Q}_1 \neq 0$, $\mathcal{Q}_2 \neq 0$, $\Delta = (\mathcal{Q}_2^2 - 4\mathcal{Q}_1) = 0$, $\mathcal{P}_2 = 0$,

$$\mathcal{E}_3 = a_0 + \frac{\mathcal{Q}_2^2\left(-a_1\left(\frac{1}{C+b_3 s - b_4 t + x + b_1 y + b_2 z} + \mathcal{Q}_2\right) - \mathcal{Q}_2^2\right)}{2\left(\frac{1}{C+b_3 s - b_4 t + x + b_1 y + b_2 z} + \mathcal{Q}_2\right)^2}. \tag{27}$$

Case 4: When $(\mathcal{P}_1\mathcal{P}_4 - \mathcal{P}_2\mathcal{P}_3) \neq 0$, $\mathcal{Q}_1 \neq 0$, $\mathcal{Q}_2 \neq 0$, $\Delta = (\mathcal{Q}_2^2 - 4\mathcal{Q}_1) = 0, \mathcal{P}_3 = 0$,

$$\mathcal{E}_6 = a_0 + \frac{\mathcal{Q}_2^2\left(a_1\left(\frac{1}{C+b_3 s - b_4 t + x + b_1 y + b_2 z} + \mathcal{Q}_2\right) - \mathcal{Q}_2^2\right)}{2\left(\frac{1}{C+b_3 s - b_4 t + x + b_1 y + b_2 z} + \mathcal{Q}_2\right)^2}. \tag{28}$$

Case 5: When $(\mathcal{P}_1\mathcal{P}_4 - \mathcal{P}_2\mathcal{P}_3) \neq 0$, $\mathcal{Q}_1 < 0$, $\mathcal{Q}_2 = 0$,

$$\mathcal{E}_{10} = a_0 + \frac{a_1\left(e^{2\sqrt{-\mathcal{Q}_1}(C+\chi)} - \sqrt{-\mathcal{Q}_1}\right)}{e^{2\sqrt{-\mathcal{Q}_1}(C+\chi)} + 1} - \frac{2\left(\sqrt{-\mathcal{Q}_1} - e^{2\sqrt{-\mathcal{Q}_1}(C+\chi)}\right)^2}{\left(e^{2\sqrt{-\mathcal{Q}_1}(C+\chi)} + 1\right)^2}, \tag{29}$$

where $\chi = x + b_1 y + b_2 z + b_3 s - b_4 t$.

4. Results and Insights

Here, we explore the physical traits and present solutions to examine the characteristics of the (4+1)-D KdV-CBS equation. By applying the GEM, we developed a series of visual representations for various parameter values, which are essential for identifying exact soliton solutions across a wide range of governing models. Using Mathematica 13, we generate graphical depictions of these new traveling wave solutions, which contain trigonometric, rational, and hyperbolic functions. These strategies, previously unexplored within this specific governing model, present significant progress in generating soliton solutions. We simulate the exact solitary wave patterns for $[\mathcal{E}_1(x,t)]$, $[\mathcal{E}_2(x,t)]$, $[\mathcal{E}_3(x,t)]$, $[\mathcal{E}_6(x,t)]$, and $[\mathcal{E}_{10}(x,t)]$, incorporating 3D, 2D, and contour visualizations to illustrate the behavior under selected parameter values.

For instance, by applying specific parameters from Equation (25) such as $C = 1$, $b_2 = 1$, $b_1 = 2$, $b_4 = -1$, $b_3 = 1$, $Q_2 = -0.5$, $Q_1 = 0.01$, $a_0 = 1$, $a_1 = 1$, $s = 1$, $y = 1$, and $z = 1$, we assessed the physical characteristics of $[\mathcal{E}_1(x,t)]$, as shown in Figure 1a–c, which illustrates the interaction of bright solitons. Similarly, with the parameters from Equation (26), including $C = 1$, $b_2 = 1$, $b_1 = 2$, $b_4 = -1$, $b_3 = 1$, $Q_2 = -0.5$, $Q_1 = 1$, $a_0 = 1$, $a_1 = 0.1$, $s = 1$, $y = 1$, and $z = 1$, we examined the physical characteristics of $[\mathcal{E}_2(x,t)]$. Figure 2a–c depict periodic singular solitary waves. Further, using parameters from Equation (27), such as $C = 1$, $b_2 = 1$, $b_1 = 2$, $b_4 = -1$, $b_3 = 1$, $Q_2 = -0.5$, $Q_1 = 0.25$, $a_0 = 1$, $a_1 = 2$, $s = 1$, $y = 1$, and $z = 1$, we explored the physical characteristics of $[\mathcal{E}_3(x,t)]$, as displayed in Figure 3a–c showcasing singular solitary waves. Additionally, by applying the parameters from Equation (28), including $C = 1$, $b_2 = 1$, $b_1 = 2$, $b_4 = -1$, $b_3 = 1$, $Q_2 = -0.5$, $Q_1 = 1$, $a_0 = 1$, $a_1 = 4$, $s = 1$, $y = 1$, $z = 1$, $\mathcal{P}_1 = 1$, $\mathcal{P}_2 = 1$, and $\mathcal{P}_4 = 1$, we analyzed the physical characteristics of $[\mathcal{E}_6(x,t)]$. Figure 4a–c illustrate exponential solitary waves. Finally, with

parameters from Equation (29), such as $C = 1$, $b_2 = 1$, $b_1 = 2$, $b_4 = -1$, $b_3 = 1$, $Q_2 = 0$, $Q_1 = -1$, $a_0 = 1$, $a_1 = 0$, $s = 1$, $y = 1$, $z = 1$, $\mathcal{P}_1 = 1$, $\mathcal{P}_2 = 1$, and $\mathcal{P}_4 = 1$, we evaluated the physical characteristics of $[\mathcal{E}_{10}(x,t)]$. Figure 5a–c display the interaction of singular solitary waves.

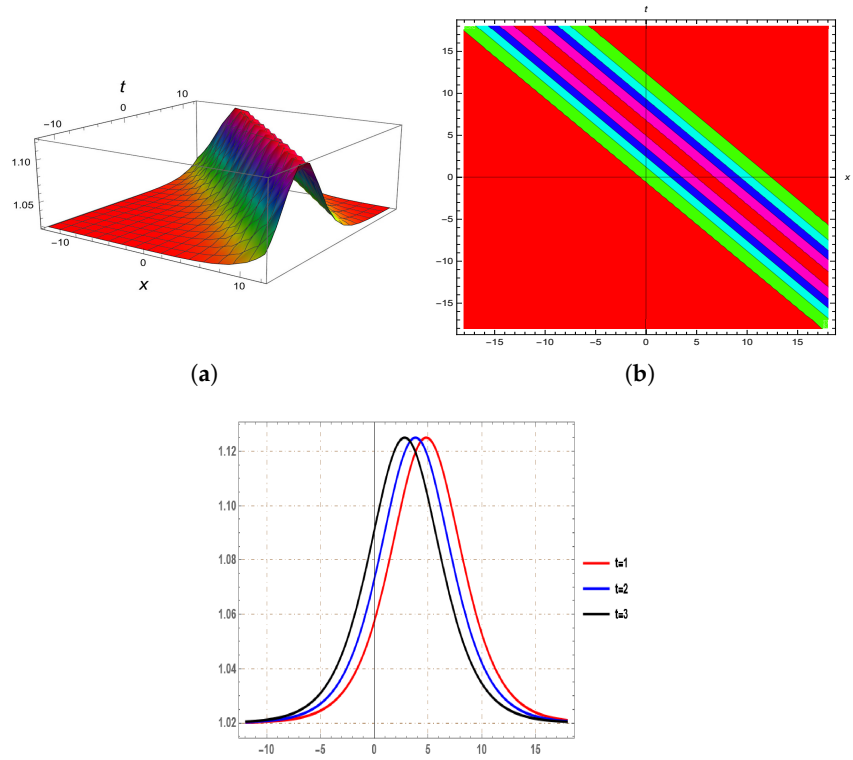

(**a**) (**b**)

(**c**)

Figure 1. Figure (**a**) shows the 3D visualization, (**b**) the contour plot, and (**c**) the 2D view of $[\mathcal{E}_1(x,t)]$.

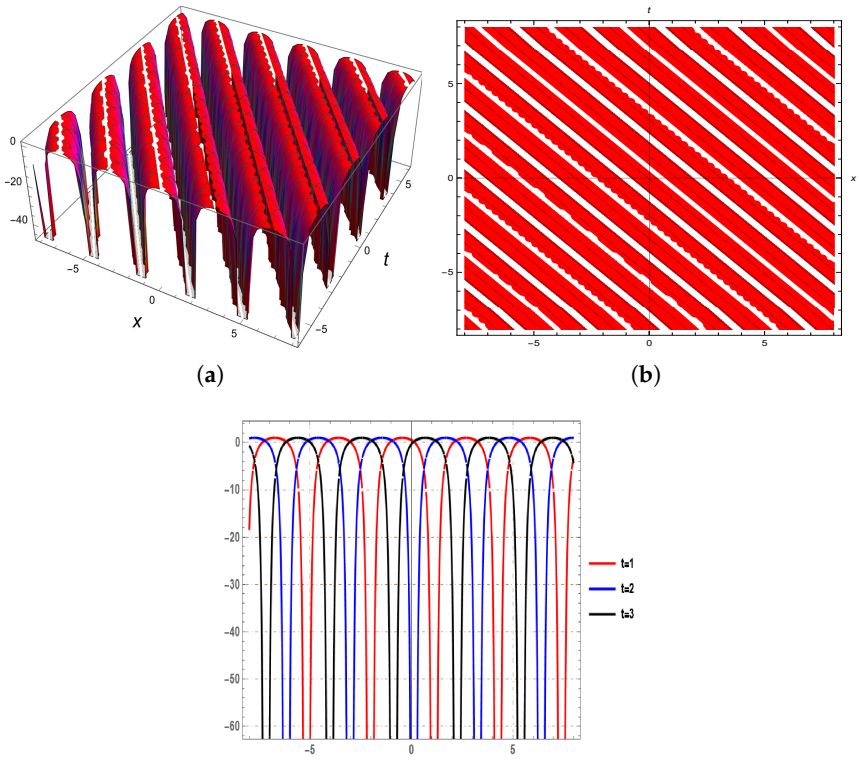

(**a**) (**b**)

(**c**)

Figure 2. Figure (**a**) shows the 3D visualization, (**b**) the contour plot, and (**c**) the 2D view of $[\mathcal{E}_2(x,t)]$.

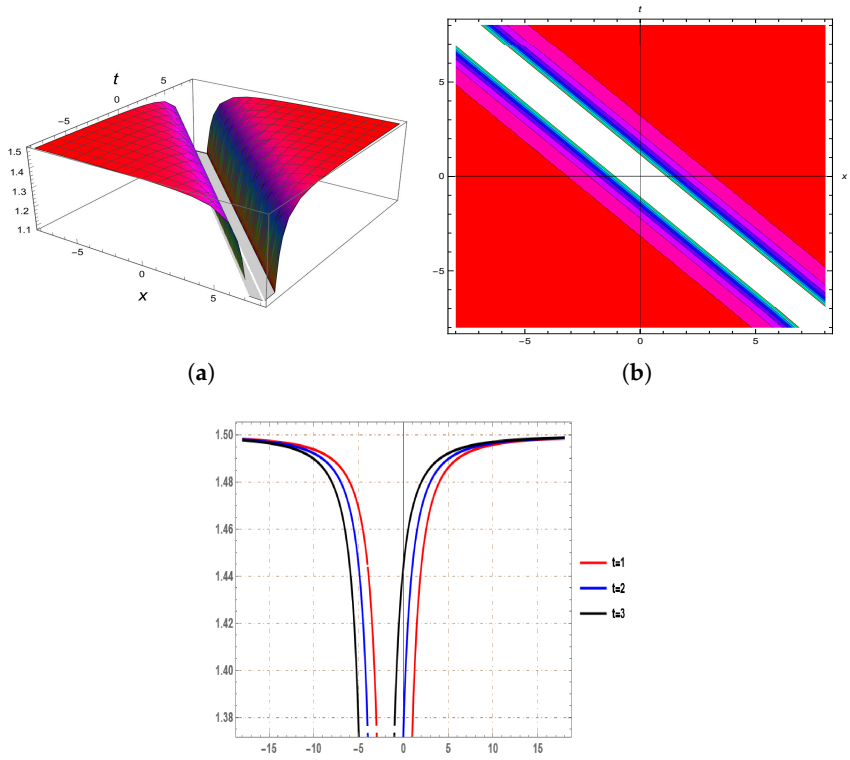

(**a**) (**b**)

(**c**)

Figure 3. Figure (**a**) shows the 3D visualization, (**b**) the contour plot, and (**c**) the 2D view of $[\mathcal{E}_3(x,t)]$.

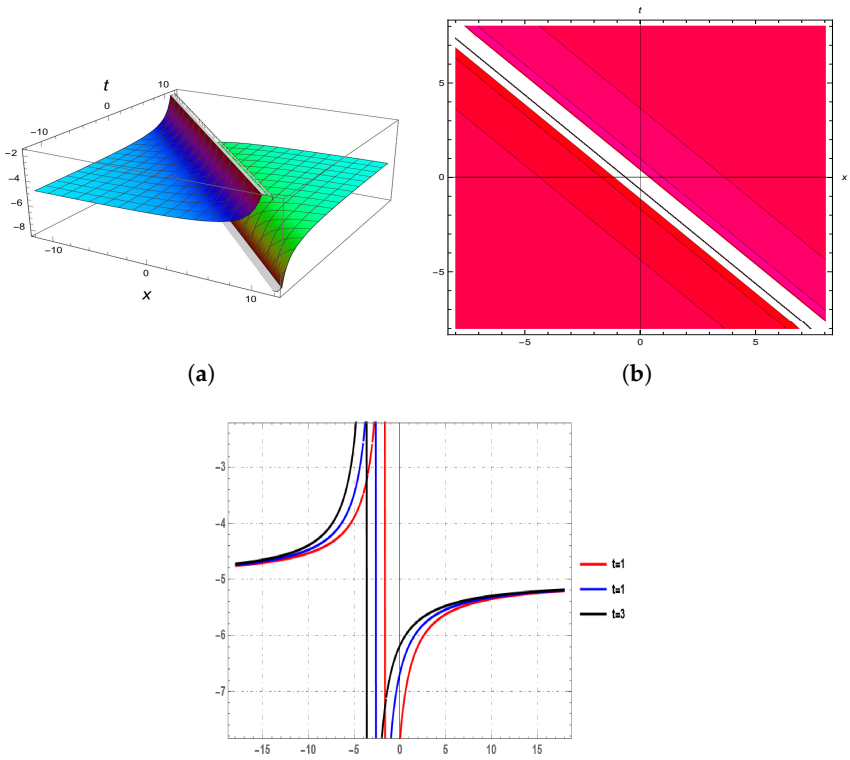

(**a**) (**b**)

(**c**)

Figure 4. Figure (**a**) shows the 3D visualization, (**b**) the contour plot, and (**c**) the 2D view of $[\mathcal{E}_6(x,t)]$.

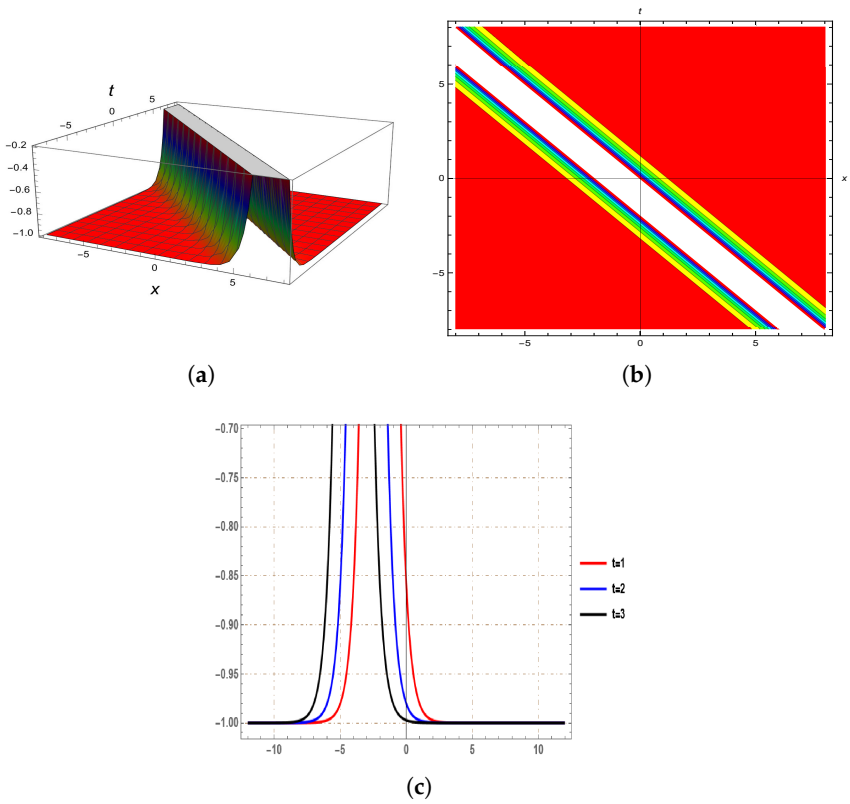

(**a**) (**b**)

(**c**)

Figure 5. Figure (**a**) shows the 3D visualization, (**b**) the contour plot, and (**c**) the 2D view of $[\mathcal{E}_{10}(x,t)]$.

5. Qualitative Evaluation

Here, we explore the bifurcation analysis of the given nonlinear equation. By using the above-mentioned transformation, we convert the system into an ODE, and Equation (7) can be rewritten as follows:

$$2\mathcal{F}'\mathcal{F}'' + 6\mathcal{F}^2\mathcal{F}' - 2\mathcal{F}\mathcal{F}'A - \mathcal{F}'B = 0. \tag{30}$$

We apply bifurcation theory to Equation (30), which can be formulated as a planar dynamical system through the use of the Galilean transformation:

$$\begin{cases} \frac{d\mathcal{F}}{d\chi} = \wedge, \\ \frac{d\wedge}{d\chi} = -3\mathcal{F}^2 + \mathcal{F}A + \frac{B}{2}, \end{cases} \tag{31}$$

where $A = \frac{bb_1+cb_2+db_3+a-4b_4}{\alpha b_1+\beta b_2+\gamma b_3+\epsilon}$, and $B = \frac{2C_2}{\alpha b_1+\beta b_2+\gamma b_3+\epsilon}$. It constitutes a Hamiltonian system; the associated integral is expressed as follows:

$$E = \frac{\wedge^2}{2} + F^3 - \frac{A}{2}F^2 - \frac{B}{2}F.$$

We now examine the bifurcations of System (31) through phase portraits in terms of parameters A and B. Our qualitative analysis revealed the following key findings: Firstly, it is important to note the two fixed points that exist in System (31):

$$G_1 = (\frac{A+\sqrt{A^2+6B}}{6}, 0) \text{ and } G_2 = (\frac{A-\sqrt{A^2+6B}}{6}, 0).$$

Furthermore, the Jacobian of the system is given by the following:

$$J(\mathcal{F}, \wedge) = \begin{vmatrix} 0 & 1 \\ -6\mathcal{F} + A & 0 \end{vmatrix} = 6\mathcal{F} - A \neq 0. \tag{32}$$

Thus, we have the following:

$J(\mathcal{F}, \wedge) > 0$ is the center point;
$J(\mathcal{F}, \wedge) < 0$ is the saddle point;
$J(\mathcal{F}, \wedge) = 0$ is the cuspidal point.

To assess stability, the eigenvalues of the Jacobian matrix are typically evaluated at fixed points G_1 and G_2.

$$\lambda_{\pm} = \frac{1}{2}\left(tra(J) \pm \sqrt{(tra(J))^2 - 4det(J)}\right).$$

The parameters A and B govern the system, where the condition $A^2 + 6B$ represents the merging of fixed points G_1 and G_2, leading to a saddle-center bifurcation and phase space transformations.

The following results are achievable by setting the relevant parameters to varied values.

Case 1: $A^2 + 6B > 0$
For $B = 1$, setting $A = 2.5$, two equilibrium points are identified as $G_1 = (1, 0)$ and $G_2 = (-0.1667, 0)$, extracted from System (31). G_1 is the center point, while G_2 displays the saddle point as shown in Figure 6.

Case 2: $A^2 + 6B < 0$
Our discussion focuses solely on the real equilibrium points; however, in the following case, there are no real solutions for G_1 and G_2.

Case 3: $A^2 + 6B = 0$
One equilibrium point from System (31) was retrieved using $A = \sqrt{6}$ and $B = -1$. $G_1 = G_2 = (0.4082, 0)$ displays a cusp, as can be seen in Figure 7.

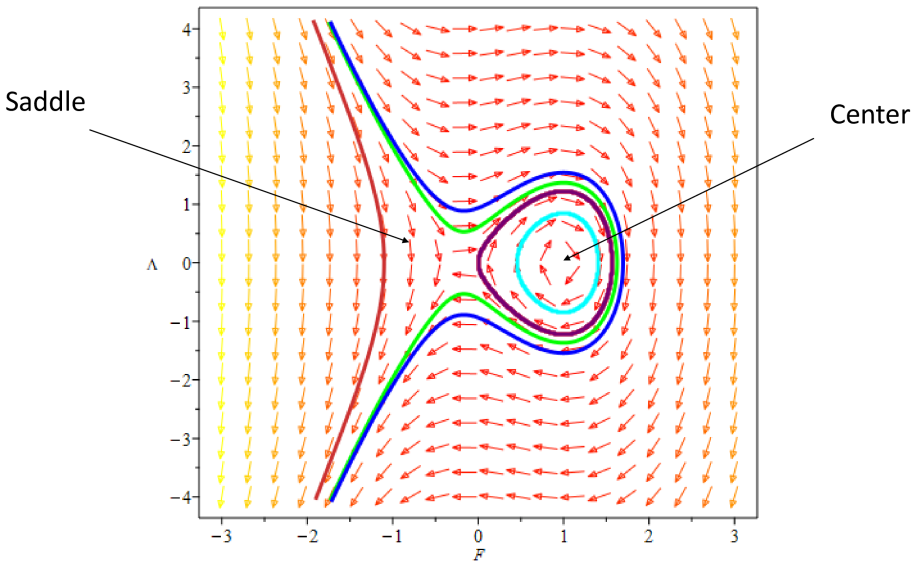

Figure 6. Bifurcation analysis for $A^2 + 6B > 0$ with $B = 1$ and $A = 2.5$.

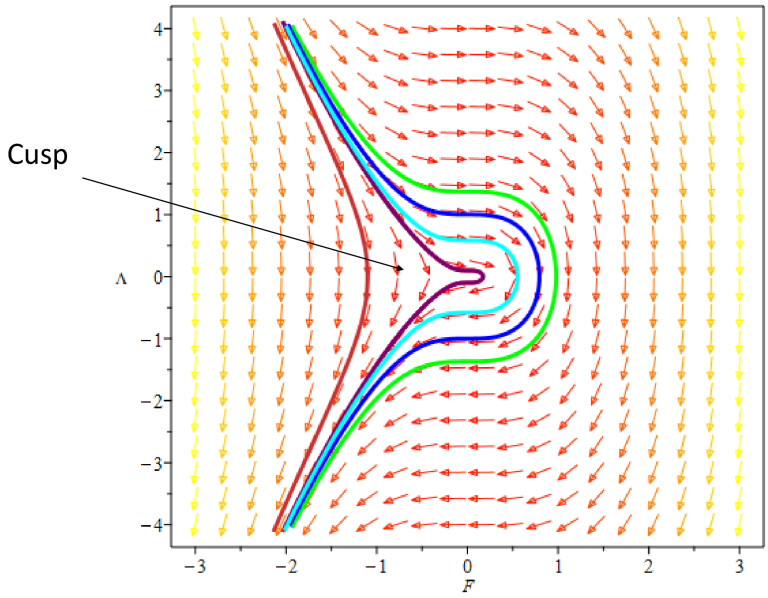

Figure 7. Bifurcation analysis for $A^2 + 6B = 0$ with $A = \sqrt{6}$ and $B = -1$.

6. Chaotic Behavior

Although a dynamical system may be inherently deterministic, chaotic behavior in its trajectory over time reflects unpredictability and disorder. Non-repeating paths, complex patterns in phase space, and high sensitivity to initial conditions characterize chaotic dynamics. Small alterations in the initial conditions can result in radically different outcomes, making long-term predictions impossible. To comprehend the chaotic behavior dynamics of the mentioned equation, we must include the perturbation term in System (31), which becomes as follows:

$$\begin{cases} \frac{d\mathcal{F}}{d\chi} = \wedge, \\ \frac{d\wedge}{d\chi} = -3\mathcal{F}^2 + \mathcal{F}A + \frac{B}{2} + \varsigma_0 cos(\sigma\chi). \end{cases} \tag{33}$$

The external force acting on the model is indicated by the parameters ς_0 and σ in (33). Adding $\cos(\sigma\chi)$ as a perturbation allows for a detailed investigation of periodic forcing effects on the system's trajectories. Chaos in a dynamical system's ODE reflects the complex behavior of its corresponding NLPDE when reduced to finite dimensions. Nonlinearity and instabilities in the NLPDE persist in the reduced system, linking spatiotemporal and temporal chaos [29]. Chaotic behavior within the governing model can be demonstrated using chaos detection methods such as bifurcation diagrams, time series analysis, phase portraits, Poincaré maps, and Lyapunov exponents.

Time series: Data points gathered over an extended period of time are referred to as time series. Recording the values of various parameters at regular intervals is necessary while observing state variables. Through time series analysis, we may identify dependencies, patterns, and trends in the data, helping us to comprehend how the variables evolve with time.

Phase portrait: A phase portrait in chaos theory is a visual representation of how a dynamical system behaves over time, showing the paths of its state variables in phase space. If we look closely at these pictures, we can see important details like attractor and repellent qualities. They also provide additional details on the dynamics of the system, such as whether they are chaotic or behave regularly, and the stability of the system.

Poincaré map: You can investigate the time behaviors of dynamical systems by looking at their intersections with specific hyperplanes through the Poincaré map. This helps

distinguish between chaotic areas, periodic orbits, and unstable and stable manifolds by giving a condensed picture of the system's motions.

Bifurcation diagram: A bifurcation diagram is a helpful tool that shows how a dynamical system's behavior changes when you tweak a certain parameter. It illustrates the many behaviors that arise when the system experiences bifurcations, including stable fixed points, periodic orbits, and chaotic patterns.

Lyapunov exponents: The Lyapunov exponent in chaos theory measures how quickly nearby paths in a dynamical system either spread apart or come together. When the exponent is positive, paths that start close to each other move away rapidly, showing chaotic behavior. On the other hand, negative exponents suggest stability, as nearby trajectories come closer over time. This measure gives a straightforward way to gauge how sensitive and predictable a chaotic system is based on its starting conditions. The graphs of these phenomena for the governing model has been shown as Figures 8–12.

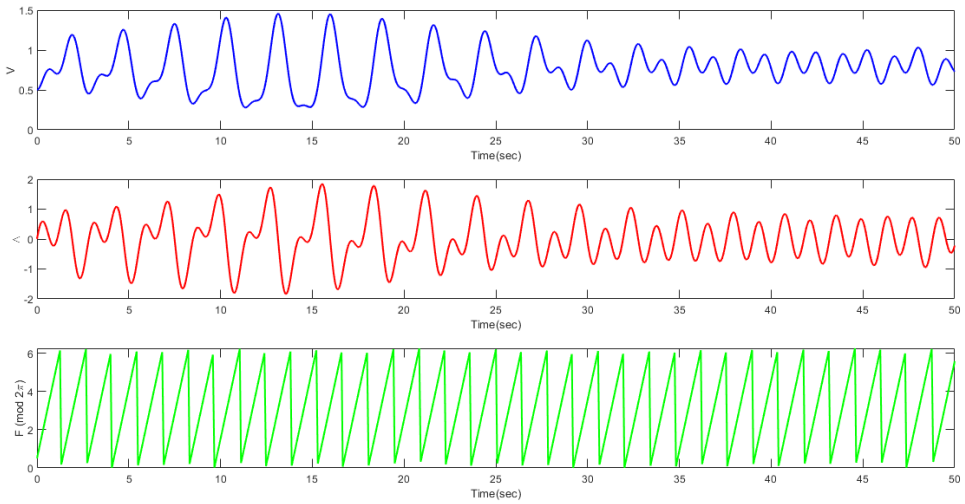

Figure 8. Chaotic behavior is detected using time series when $A = -0.01$, $B = 1$, $\varsigma_0 = 2.5$, $\chi = 4.5$, and satisfies $I.C = [0.5, 0, 0.5]$.

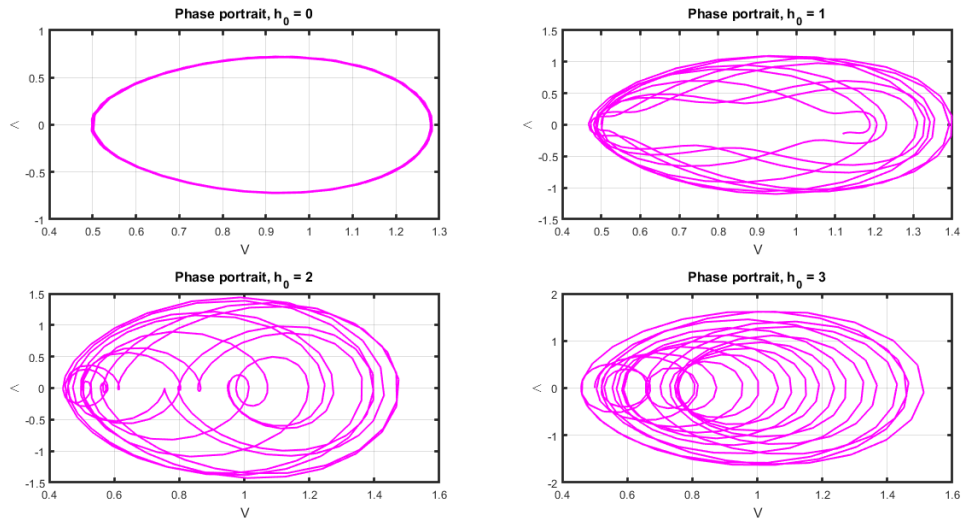

Figure 9. Chaotic behavior is detected using phase portrait when $A = 2$, $B = 1.5$, $\varsigma_0 = [0, 1, 2, 3]$, $\chi = 4$, and satisfies $I.C = [0.5, 0, 0.5]$.

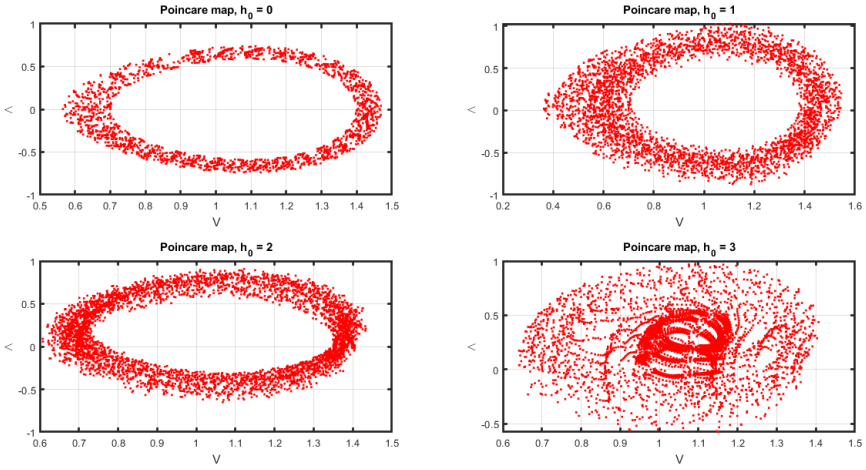

Figure 10. Chaotic behavior is detected using the Poincaré map when $A = 3.5$, $B = -0.5$, $\varsigma_0 = [0, 1, 2, 3]$, $\chi = 4$, and satisfies $I.C = [0.7, 0, 0.7]$.

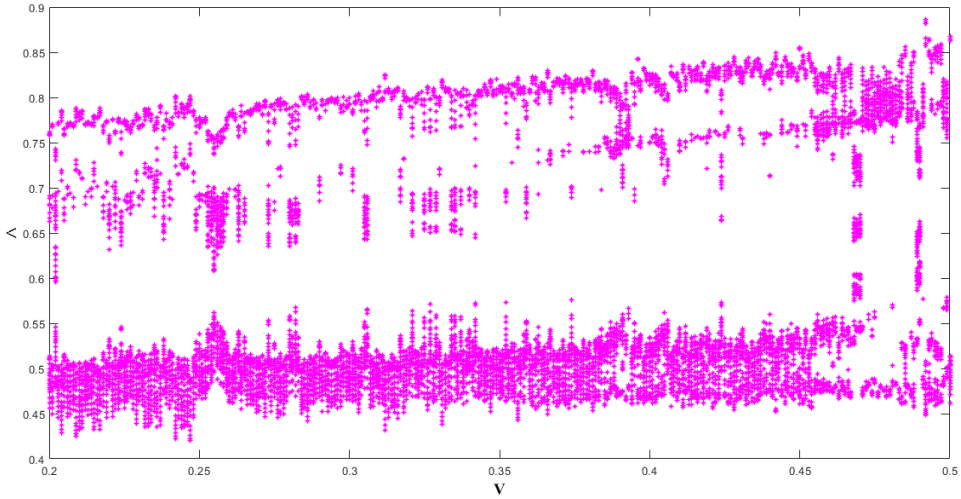

Figure 11. Chaotic behavior is detected using the bifurcation diagram when $A = 2$, $B = 7.5$, $\varsigma_0 = 1.5$, $\chi = 4$, and satisfies $I.C = [0.5, 0, 0.5]$.

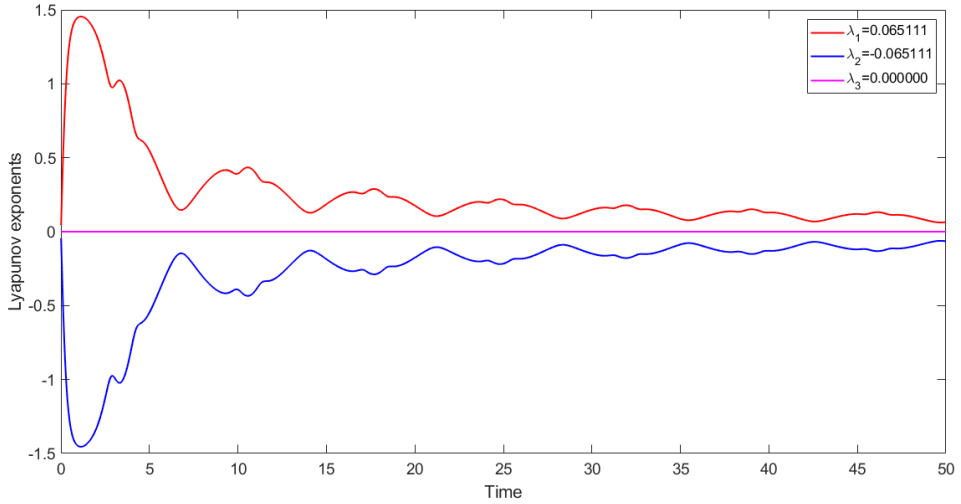

Figure 12. Chaotic behavior is detected using the Lyapunov exponent when $A = 0.09$, $B = 1.2$, $\varsigma_0 = -0.01$, $\chi = 11$, and satisfies $I.C = [-0.4, 0, -0.4]$.

7. Sensitivity Analysis

This section looks into the sensitivity analysis of System (31) under three different initial conditions. The curves for the two and three solutions are examined and contrasted, as depicted in Figures 13–15, with parameter values $A = -1.5$ and $B = 1$. A comparative analysis was conducted at various initial conditions, as illustrated in Figure 16, including $(0.1, 0)$, $(0.2, 0)$, and $(0.3, 0)$. It can be seen that a small variation in the starting values results in a significant variation in the solution. As a result, we now reach the sensitive part of the model.

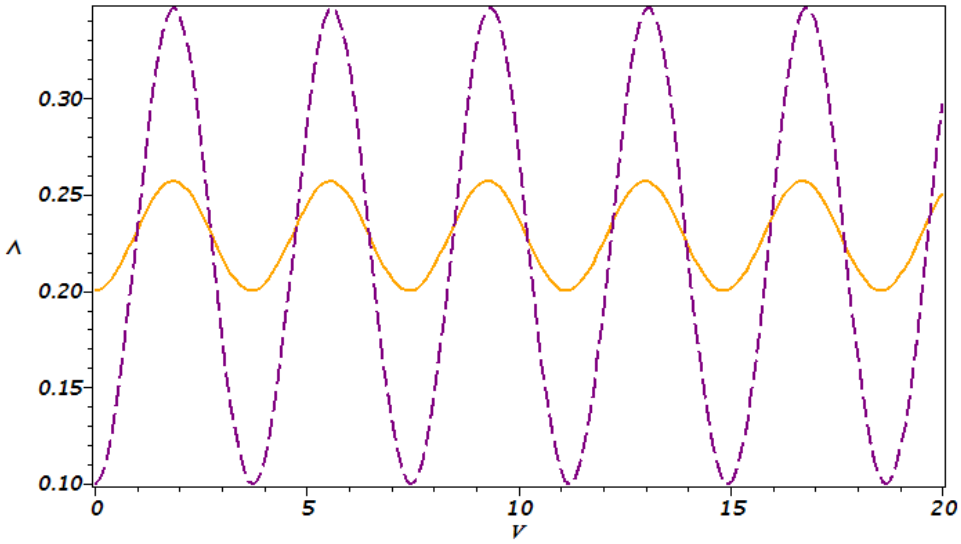

Figure 13. Sensitivity plots for (31) with two initial conditions: $(\mathcal{F}, \wedge) = (0.1, 0)$ and $(\mathcal{F}, \wedge) = (0.2, 0)$.

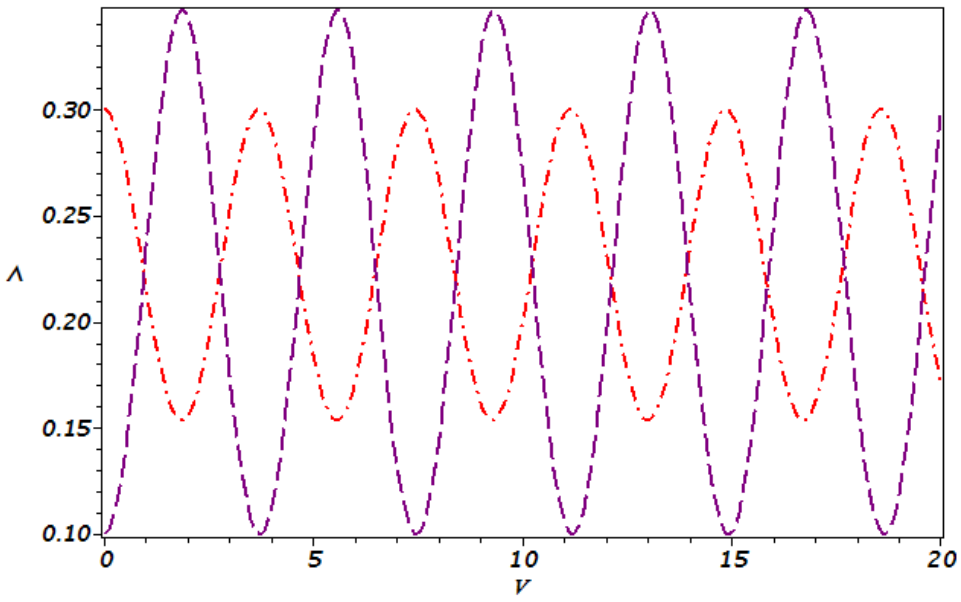

Figure 14. Sensitivity plots for (31) with two initial conditions: $(\mathcal{F}, \wedge) = (0.1, 0)$ and $(\mathcal{F}, \wedge) = (0.3, 0)$.

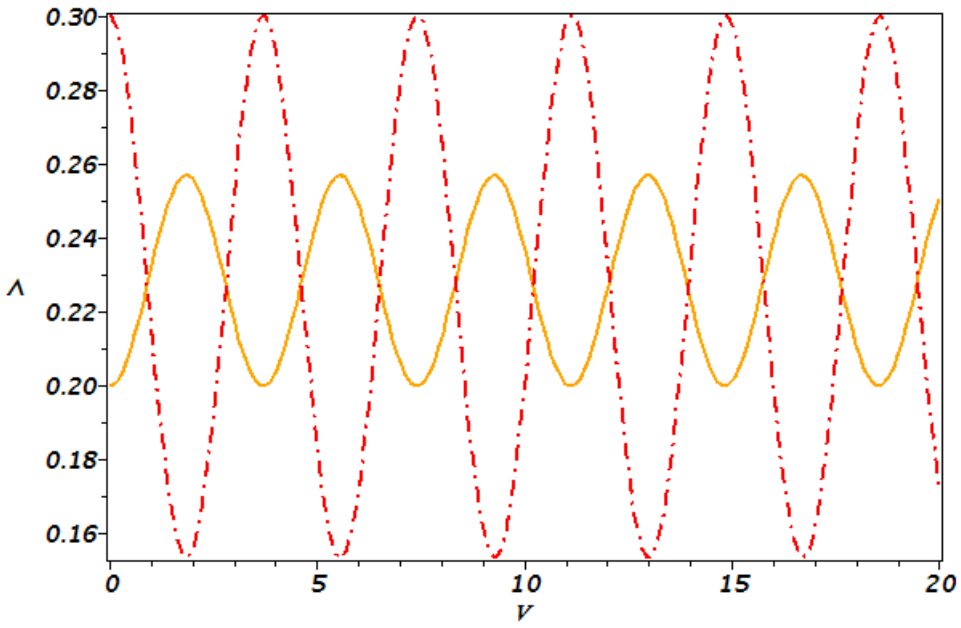

Figure 15. Sensitivity plots for (31) with two initial conditions: $(\mathcal{F}, \wedge) = (0.2, 0)$ and $(\mathcal{F}, \wedge) = (0.3, 0)$.

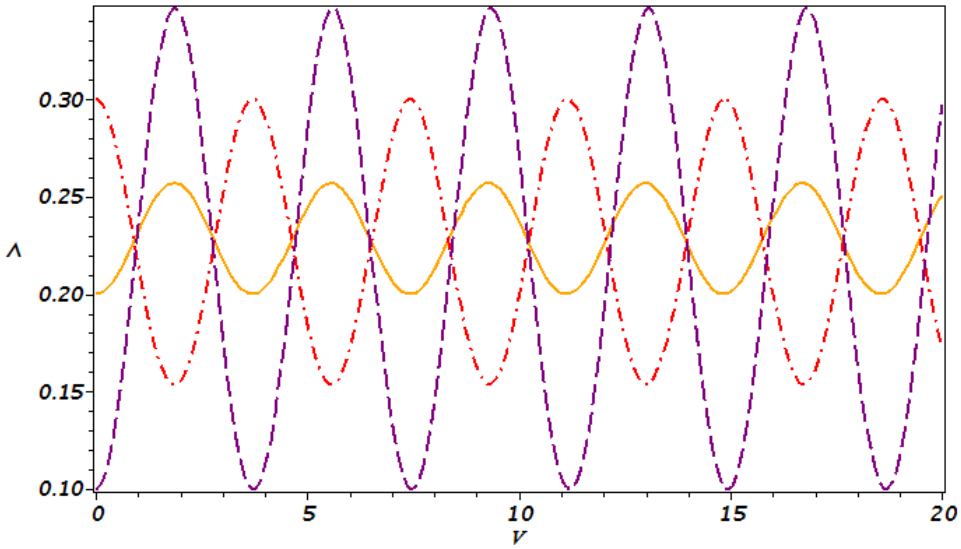

Figure 16. Sensitivity plots for (31) with two initial conditions: $(\mathcal{F}, \wedge) = (0.1, 0)$, $(\mathcal{F}, \wedge) = (0.2, 0)$ and $(\mathcal{F}, \wedge) = (0.3, 0)$.

8. Conclusions and Future Directions

In this manuscript, we present novel soliton solutions for the (4+1)-D KdV-CBS equation. By employing the GEM, we derived a variety of solitary wave solutions, including those with rational, exponential, hyperbolic, and trigonometric functions. The inclusion of arbitrary parameters in these solutions allows for a wide range of optical soliton types, including singular, periodic, bright, rational, and novel solitary waves. The visual representations in 3D, 2D, and contour formats provide a comprehensive view of our results. Our approach is distinguished by its innovative application of new methodologies, leading to the discovery of diverse optical soliton solutions. We also examined the dynamic behavior of the equation by analyzing bifurcations at equilibrium points. By applying a Galilean transformation, we transformed the governing system into a planar dynamic system and conducted a qualitative analysis, with bifurcation results depicted through phase portraits. Additionally, we performed a sensitivity analysis illustrating the system's behavior under various initial conditions through detailed graphs. Our calibration of solutions with spe-

cific parameter values highlights the effectiveness of our approach in addressing nonlinear problems relevant to fields such as astrophysics, space research, laboratory studies, and technology. Future work is anticipated to further investigate higher-dimensional integrable systems with potential physical applications, building upon the insights gained from this study.

Author Contributions: Conceptualization, N.R.; Methodology, M.L.G.; Software, M.U.; Validation, N.R.; Formal analysis, M.L.G.; Investigation, M.U. and Y.A.; Resources, Y.A.; Writing—original draft, M.U.; Writing—review & editing, M.L.G., N.R. and Y.A.; Project administration, Y.A. All authors have read and agreed to the published version of the manuscript.

Funding: The authors extend their appreciation to the Deanship of Research and Graduate Studies at King Khalid University, KSA for funding this work through Large Research Project under grant number RGP.2/430/45.

Data Availability Statement: There are no associated data for our manuscript.

Acknowledgments: MLG gratefully acknowledges the support of the Junta de Andalucia FQM-201 group. The authors extend their appreciation to the Deanship of Research and Graduate Studies at King Khalid University, KSA for funding this work through Large Research Project under grant number RGP.2/430/45.

Conflicts of Interest: The authors declare that they have no conflicts of interest.

References

1. Debnath, L.; Debnath, L. *Nonlinear Partial Differential Equations for Scientists and Engineers*; Birkhäuser: Boston, MA, USA, 2005; pp. 528–529.
2. Ablowitz, M.J.; Kaup, D.J.; Newell, A.C.; Segur, H. Nonlinear-evolution equations of physical significance. *Phys. Rev. Lett.* **1973**, *31*, 125. [CrossRef]
3. Hossain, A.K.M.K.S.; Akbar, M.A. Solitary wave solutions of few nonlinear evolution equations. *AIMS Math.* **2020**, *5*, 1199–1215. [CrossRef]
4. Kaplan, M.; Hosseini, K.; Samadani, F.; Raza, N. Optical soliton solutions of the cubic-quintic non-linear Schrödinger's equation including an anti-cubic term. *J. Mod. Opt.* **2018**, *65*, 1431–1436. [CrossRef]
5. Butt, A.R.; Umair, M.; Basendwah, G.A. Exploring advanced non-linear effects on highly dispersive optical solitons with multiplicative white noise. *Optik* **2024**, *308*, 171801. [CrossRef]
6. Serkin, V.N.; Hasegawa, A. Novel soliton solutions of the nonlinear Schrödinger equation model. *Phys. Rev. Lett.* **2000**, *85*, 4502. [CrossRef] [PubMed]
7. Estévez, P.G.; Prada, J. Singular manifold method for an equation in 2+1 dimensions. *J. Nonlinear Math. Phys.* **2005**, *12* (Suppl. S1), 266–279. [CrossRef]
8. Hafez, M.G.; Akbar, M.A. An exponential expansion method and its application to the strain wave equation in microstructured solids. *Ain Shams Eng. J.* **2015**, *6*, 683–690. [CrossRef]
9. Zayed, E.M.; Shohib, R.M.; Al-Nowehy, A.G. Solitons and other solutions for higher-order NLS equation and quantum ZK equation using the extended simplest equation method. *Comput. Math. Appl.* **2018**, *76*, 2286–2303. [CrossRef]
10. Korteweg, D.J.; De Vries, G. XLI. On the change of form of long waves advancing in a rectangular canal, and on a new type of long stationary waves. *Lond. Edinb. Dublin Philos. Mag. J. Sci.* **1895**, *39*, 422–443. [CrossRef]
11. Olver, P.J. Evolution equations possessing infinitely many symmetries. *J. Math. Phys.* **1977**, *18*, 1212–1215. [CrossRef]
12. Khuri, S.A. Soliton and periodic solutions for higher order wave equations of KdV type (I). *Chaos Solitons Fractals* **2005**, *26*, 25–32. [CrossRef]
13. Bogoyavlenskiĭ, O.I. Overturning solitons in new two-dimensional integrable equations. *Math. USSR-Izv.* **1990**, *34*, 245. [CrossRef]
14. Schiff, J. Integrability of Chern-Simons-Higgs vortex equations and a reduction of the self-dual Yang-Mills equations to three dimensions. In *Painlevé Transcendents: Their Asymptotics and Physical Applications*; Springer: Boston, MA, USA, 1992; pp. 393–405.
15. Toda, K.; Yu, S.J. The investigation into the Schwarz–Korteweg–de Vries equation and the Schwarz derivative in (2+1) dimensions. *J. Math. Phys.* **2000**, *41*, 4747–4751. [CrossRef]
16. Li, Y.; Chaolu, T. Exact solutions for (2+1)-dimensional KdV-Calogero-Bogoyavlenkskii-Schiff equation via symbolic computation. *J. Appl. Math. Phys.* **2020**, *8*, 197. [CrossRef]

17. Qin, C.Y.; Tian, S.F.; Zou, L.; Ma, W.X. Solitary wave and quasi-periodic wave solutions to a (3+1)-dimensional generalized Calogero–Bogoyavlenskii–Schiff equation. *Adv. Appl. Math. Mech* **2018**, *10*, 948–977.
18. Hirota, R.; Satsuma, J. N-soliton solutions of model equations for shallow water waves. *J. Phys. Soc. Jpn.* **1976**, *40*, 611–612. [CrossRef]
19. Xu, G.Q.; Liu, Y.P.; Cui, W.Y. Painlevé analysis, integrability property and multiwave interaction solutions for a new (4+1)-dimensional KdV–Calogero–Bogoyavlenkskii–Schiff equation. *Appl. Math. Lett.* **2022**, *132*, 108184. [CrossRef]
20. Wazwaz, A.M. Two new Painlevé integrable KdV–Calogero–Bogoyavlenskii–Schiff (KdV-CBS) equation and new negative-order KdV-CBS equation. *Nonlinear Dyn.* **2021**, *104*, 4311–4315. [CrossRef]
21. Chahlaoui, Y.; Umair, M.; Butt, A.R.; Alshahrani, A.A. Modulation instability and extraction of fractional optical solitons in the presence of generalized Kudryashov's law and dual form of non-local nonlinearity. *Phys. Scr.* **2024**, *99*, 075226. [CrossRef]
22. Shakeel, M.; Attaullah; El-Zahar, E.R.; Shah, N.A.; Chung, J.D. Generalized exp-function method to find closed form solutions of nonlinear dispersive modified Benjamin–Bona–Mahony equation defined by seismic sea waves. *Mathematics* **2022**, *10*, 1026. [CrossRef]
23. Raza, N.; Kazmi, S.S.; Basendwah, G.A. Dynamical analysis of solitonic, quasi-periodic, bifurcation and chaotic patterns of Landau–Ginzburg–Higgs model. *J. Appl. Anal. Comput.* **2024**, *14*, 197–213. [CrossRef] [PubMed]
24. Kuznetsov, E.A.; Dias, F. Bifurcations of solitons and their stability. *Phys. Rep.* **2011**, *507*, 43–105. [CrossRef]
25. Hosseini, K.; Hinçal, E.; Ilie, M. Bifurcation analysis, chaotic behaviors, sensitivity analysis, and soliton solutions of a generalized Schrödinger equation. *Nonlinear Dyn.* **2023**, *111*, 17455–17462. [CrossRef]
26. Jhangeer, A.; Raza, N.; Ejaz, A.; Rafiq, M.H.; Baleanu, D. Qualitative behavior and variant soliton profiles of the generalized P-type equation with its sensitivity visualization. *Alex. Eng. J.* **2024**, *104*, 292–305. [CrossRef]
27. Sjöberg, A. On double reductions from symmetries and conservation laws. *Nonlinear Anal. Real World Appl.* **2009**, *10*, 3472–3477. [CrossRef]
28. Anco, S.C.; Gandarias, M.L. Symmetry multi-reduction method for partial differential equations with conservation laws. *Commun. Nonlinear Sci. Numer. Simul.* **2020**, *91*, 105349. [CrossRef]
29. Wiggins, S. *Introduction to Applied Nonlinear Dynamical Systems and Chaos*; Electronic Resource; Springer: New York, NY, USA, 2003.